Influence of graphene nanoplatelets on curing and mechanical properties of graphene/epoxy nanocomposites

M. G. Prolongo[1] · C. Salom[1] · C. Arribas[1] · M. Sánchez-Cabezudo[1] · R. M. Masegosa[1] · S. G. Prolongo[2]

Abstract The influence of graphene nanoplatelets (GNPs) on the curing of an epoxy resin based on diglycidyl ether of bisphenol A (DGEBA) and cross-linked with 4,4′-diaminodiphenylmethane (DDM) was studied. Dynamic mechanical properties and tensile properties of the corresponding graphene/epoxy nanocomposites were obtained. Two compositions 1 and 5 mass% of GNPs were studied. The cross-linking reaction of the epoxy resin is accelerated in dispersions with 5 mass% GNPs. In the presence of GNPs, the curing reaction becomes less exothermic, obtaining less perfect epoxy networks compared to neat epoxy (DGEBA–DDM) thermoset. Accordingly, the glass transition temperatures (T_g) of the nanocomposites are lower than that of the neat epoxy thermoset. This effect is not detected for low content of graphene (1 mass%). Protocol of curing having two isothermal steps leads to more perfect networks than the dynamic curing in the DSC. The T_g reduction is minimized in the samples cured through two isothermal steps. The storage moduli of the nanocomposite containing 5 mass% graphene, both in the glassy ($T < T_g$) and the rubbery ($T > T_g$) states, are higher than the ones of neat epoxy thermoset, being most pronounced this effect at $T > T_g$. Tensile tests confirmed the higher elastic moduli of the nanocomposites; however, a decrease in strain at break and tensile strength was observed for the nanocomposite containing 5 mass% of GNPs. This brittle behavior is consistent with the morphology of the samples studied by scanning electron microscopy.

Keywords Graphene · Epoxy · Nanocomposites · Curing · Glass transition · Mechanical properties

Introduction

Epoxy thermosets have characteristics such as high chemical and solvent resistance, creep resistance, heat resistance, low shrinkage on curing, good mechanical properties and excellent adhesion to metals and ceramics, so they are widely used in many applications such as adhesives, coatings and composite matrices.

Since the discovery of graphene, its use as nanoreinforcement of polymers to form nanocomposites has attracted great interest. Graphene nanoplatelets (GNPs) dispersed in a polymer matrix can lead to significant improvements in the properties and even give new features. Specifically, graphene/polymer nanocomposites may achieve high thermal and electrical conductivity and high thermal and hydrothermal resistance, increase the hydrophobicity and microwave absorption and decrease gas permeation [1, 2]. Moreover, using graphene nanoplatelets as polymer reinforcement has the advantage of its low cost compared to carbon nanotubes.

Many studies of graphene/polymer nanocomposites focus on processing methods of these composites to obtain well-dispersed nanoplatelets in the polymer matrix ensuring the best properties of the composites [3–6]. For thermosetting matrices, such as epoxy, the most common method is “in situ polymerization” which consists in mixing the graphene with the monomer or pre-polymer to

form a well-dispersed mixture that is later polymerized by adding the curing agent at suitable temperature [2].

Regarding the properties of composites with epoxy matrix, it is known that the curing process is critical in defining the properties of the composites [7, 8]. It is therefore interesting to explore the influence that GNPs can cause in curing of graphene/epoxy dispersions and the influence of different curing protocols on the properties of the GNP/epoxy nanocomposites. In this work, the curing of dispersions of GNPs in an epoxy resin and the mechanical properties of the nanocomposites obtained after curing are studied, in order to clarify the effect of GNPs in the curing reaction and in the nanocomposite properties.

Experimental

Materials

Graphene was supplied by XG Science, under the trade name of M25, has higher purity of 99.5 % by mass and consists of nanoparticles with an average thickness of 6 nm lateral and average size 25 μm. These data provided by the manufacturer match the characterization performed in previous works [3, 4].

The epoxy resin used in this study was diglycidyl ether of bisphenol A (DGEBA) (Araldite F, Ciba) with an epoxide equivalent mass of 187 g equiv^{-1}. The curing agent was 4,4′-diaminodiphenylmethane (DDM) (Acros Organics). All samples were prepared using a stoichiometric ratio of DGEBA–DDM. Frekote (Loctite, Spain) was employed as mold release product.

Preparation of the dispersions and nanocomposites

Dispersions of graphene nanoplatelets in the epoxy resin were obtained through mechanical stirring followed by sonication. In a previous work [4], it was found that sonication produced good dispersion of the nanoparticles, although delamination in individual nanoplatelets was not completely achieved. Dispersions were prepared with two concentrations of GNPs, 1 and 5 mass%. First GNP-DGEBA dispersions were maintained at 80 °C with stirring at 300 rpm during 30 min, and then they were sonicated 60 min using a horn and a sonicator UP400S Hielscher: 0.5 s cycles with a power of 400 W and amplitude of 50 %. The temperature did not exceed 80 °C. After that, the dispersions were degassed under vacuum (40 mbar, 15 min).

Once the dispersions were obtained, the curing agent (DDM) was added at 80–85 °C and mixed for 5 min. These samples were studied by differential scanning calorimetry (DSC) in order to investigate the curing reaction. Moreover, specimens for dynamic mechanical thermal analysis (DMTA) and for tensile tests were prepared. For this purpose, after adding the DDM to the dispersions, they were poured in aluminum molds of suitable dimensions and cured in an oven following the protocol: 2 h at 120 °C + 1 h at 180 °C under atmospheric pressure.

Differential scanning calorimetry (DSC)

A Mettler Toledo mod.822e differential scanning calorimeter was used to measure the glass transition temperatures and heats of reaction. The instrument was calibrated with indium and zinc, and measurements were taken under a nitrogen atmosphere. All samples were scanned three times in the DSC instrument. The exothermic peak temperature (T_p) and the reaction enthalpy (ΔH) were obtained from the first scan (−50 to 320 °C). For each composition, several first scans were done at different heating rates from 5 to 30 °C min^{-1} in order to obtain the apparent activation energy of the curing reaction (E_a). The second and third scans were performed in the temperature range 25–250 °C at 10 °C min^{-1} to obtain the T_g of the nanocomposite formed during the first scan. A similar procedure was followed to study the unreinforced system: DGEBA–DDM. Samples of 10–20 mg were weighted in aluminum pans. The T_gs were taken at the midpoint of the heat capacity change. Two to three samples corresponding to the same composition were measured for each heating rate.

Dynamic mechanical thermal analysis (DMTA)

Dynamic mechanical thermal analysis (DMTA) of cured samples was performed in dual cantilever bending mode using a DMTA V Rheometric Scientific instrument. Measurements were taken at 1, 2, 5, 10 and 50 Hz, with temperature increasing from 30 to 220 °C at a heating rate of 2 °C min^{-1}. Specimen dimensions were 35 × 10 × 1.8 mm^3. Two to three specimens were prepared for each composition. The elastic or storage modulus (E'), the loss modulus (E'') and loss tangent (tanδ) were recorded for each frequency as a function of temperature. The maxima in tanδ-temperature curves were determined to identify the α-relaxations associated with the glass transitions.

Tensile tests

The tensile mechanical properties of the nanocomposites were determined with a MTS machine model QTest 2L with a load cell of 2 kN, using an MTS extensometer model 63411F-54. Experiments were performed at room temperature (22 °C). The specimens (140 × 10 × 1.8 mm^3) were charged at a constant speed of 1 mm min^{-1} until fracture.

The stress–strain curves were recorded for six or more samples of each composition. The average values of mechanical properties tensile modulus, tensile strength and strain to failure were calculated for each composition.

Scanning electron microscopy

Morphology of composites was studied using scanning electron microscopy. A Philips XL30 instrument and a Nova NanoSEM 230 FEI (FEG) instrument were employed with beam energy of 3–30 kV. The samples were cryogenically fractured, and the fracture surfaces of the samples were coated with a thin layer (5–10 nm) of Au (Pd).

Results and discussion

Dynamic curing of GNP/epoxy dispersions by DSC

The DSC curves of neat epoxy (DGEBA–DDM), 1 mass% graphene/epoxy dispersion and 5 mass% graphene/epoxy dispersion measured at the heating rate of 10 °C min^{-1} are shown in Fig. 1. All curves exhibit a single exothermic peak corresponding to the epoxy-amine curing reaction that occurs during the DSC scan. Table 1 shows the DSC results for the two GNP dispersions in DGEBA–DDM and for neat DGEBA–DDM mixture. It can be observed that T_{peak} increases with increasing heating rate. Lower heating rates offer longer time for chemical groups to react, and faster heating rates offer less time for the reaction. Therefore, the DSC curves shift to a higher temperature as the heating rate increases, to compensate for the reduced time.

As it can be seen in Table 1, T_{peak} values for 5 mass% GNP/DGEBA–DDM are lower than the corresponding values of DGEBA–DDM; this means that the curing reaction is accelerated in the presence of graphene. A similar catalytic behavior has also been reported for carbon nanotubes/epoxy nanocomposites [9–11]. However, this catalytic effect is not detected in samples with very low graphene content (1 mass%). Although the differences between T_{peak} of neat epoxy and T_{peak} of 1 mass% GNP/DGEBA–DDM are close to the experimental error, T_{peak} of 1 mass% GNP/DGEBA–DDM is slightly higher than T_{peak} of neat epoxy. Two opposite effects have to be considered in the curing of graphene dispersions, the steric hindrance of GNPs that impedes the mobility of the reactants increasing T_{peak} [12] and the high thermal conductivity of GNPs that can explain the accelerating effect for high GNP contents [10, 11]. The behavior of 5 mass% GNPs (T_{peak} is clearly located at lower temperature) can be attributed to the higher thermal conductivity of this sample [13].

The heat of reaction, ΔH, for each composition slightly decreases as the heating rate increases, but the changes are so small that it can be considered that ΔH is almost independent of the heating rate. It is apparent that the presence of graphene lowers ΔH, indicating that the epoxy matrix in the nanocomposites has lower cross-linking degree than in neat DGEBA–DDM. This can suggest that graphene hinders the reaction of epoxy-amine groups, leading to a less perfect network than neat DGEBA–DDM. This agrees with the T_g values of the cured samples that are lower for the

Table 1 DSC results: T_{peak} and ΔH obtained from the first DSC scan at different heating rates (β) for neat DGEBA–DDM and GNP dispersions in DGEBA–DDM

Sample	β/°C min^{-1}	T_{peak}/°C[a]	$-\Delta H$/J g $epoxy^{-1}$[b]
	From 1st scan		
DGEBA–DDM	5	143	470
	10	163	450
	15	174	430
	20	183	445
	25	190	450
	30	197	410
1 mass% GNP/ DGEBA–DDM	5	146	432
	10	166	440
	15	178	410
	20	186	410
	25	195	412
	30	202	406
5 mass% GNP/ DGEBA–DDM	5	136	420
	10	154	425
	15	165	415
	20	174	394
	25	180	392
	30	186	392

[a] Estimated error ± 1 °C

[b] Estimated error ± 20 J g^{-1}

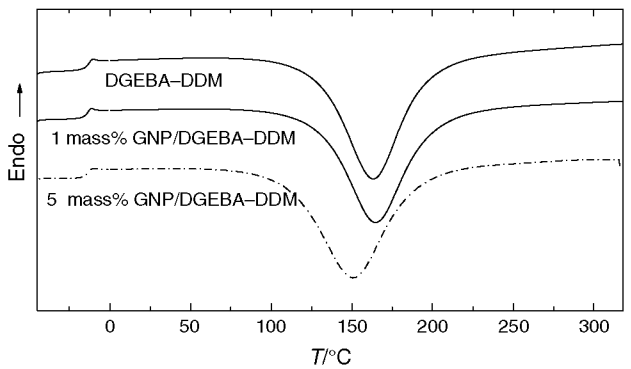

Fig. 1 DSC curves of DGEBA–DDM and of 1 mass% GNP/DGEBA–DDM and 5 mass% GNP/DGEBA–DDM dispersions at 10 °C min^{-1}

Table 2 T_g of dynamic cured samples in the DSC (−50 to 320 °C) and for samples cured in an oven (2 h 120 °C + 1 h at 180 °C), measured at 10 °C min^{-1}

Sample	T_g/°C[a] Samples cured in DSC	T_g/°C[b] Samples cured in an oven
Epoxy (DGEBA–DDM)	155	162
1 mass% GNP/DGEBA–DDM	144	162
5 mass% GNP/DGEBA–DDM	146	158

[a] Estimated error ± 1 °C

[b] Estimated error ± 0.5 °C

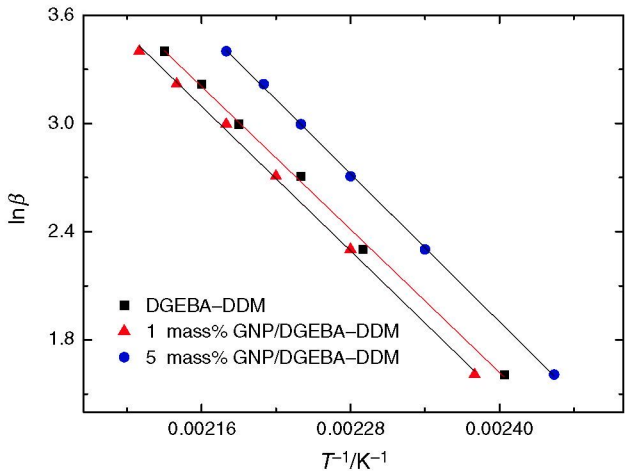

Fig. 2 Linear plot of lnβ versus T_{peak}^{-1} for the curing of DGEBA–DDM and for 1 mass% GNP/DGEBA–DDM and 5 mass% GNP/DGEBA–DDM dispersions

nanocomposites than for neat epoxy thermoset as it can be seen in Table 2.

For better understanding the effect of graphene on epoxy curing, the apparent activation energy has been obtained from the variation of T_{peak} upon heating rate (β) according to Ozawa's method [14]. Figure 2 illustrates the linear plots (lnβ vs. T_{peak}^{-1}) for DGEBA–DDM, 1 mass% GNP/DGEBA–DDM and 5 mass% GNP/DGEBA–DDM. The correlation coefficients are in the range of 0.995–0.999. The apparent activation energy of the curing reaction (E_a) obtained from the slope of the lines (slope = $-1.05\ E_a/R$) was 52.3 ± 0.9, 52.9 ± 0.9 and 54.1 ± 0.6 kJ mol^{-1} for neat DGEBA–DDM, 1 mass% GNP/DGEBA–DDM and 5 mass% GNP/DGEBA–DDM, respectively. These E_a values are in accordance with those reported in the literature for DGEBA–DDM 40–60 kJ mol^{-1} [15–17].

Although the linear fits are good, there is a risk that for the highest heating rates (25 and 30 °C min^{-1}), the samples have not reached the stated temperature at each time. Accordingly, E_a was also estimated using only the lowest heating rates (5, 10, 15 and 20 °C min^{-1}) getting similar E_a results (differences lower than 4 %). Therefore, it can be concluded that there has not been found an undoubted dependence of E_a with the content of GNPs.

The estimation of E_a by isoconversional methods yields values of E_a as a function of the conversion [18]. The method here used to evaluate E_a is not isoconversional, so the results obtained are sound only if E_a does not vary with conversion. This is a reliable assumption because as it has been reported by Zvetkov el al. [16] for DGEBA–DDM, E_a is almost constant in the range of 30–80 % conversion and at T_{peak} the conversion would be around 40–50 %.

T_g from DSC for cured GNP/epoxy nanocomposites and neat DGEBA–DDM thermoset

Two types of samples have been studied: samples cured during the first scan (−50 to 320 °C) in the DSC and samples cured in an oven following the protocol: 2 h 120 °C + 1 h at 180 °C. The T_gs were determined in the DSC instrument at 10 °C min^{-1}. Table 2 shows the obtained results. For samples cured during the first DSC scan, the heating rate used (5–30 °C min^{-1}) has no influence on their T_g determined in subsequent DSC scans. It is worth noting that the T_g values obtained from second and third scans were coincident and the corresponding scans never showed any exothermic peak; thus, the reaction was completed. Comparing the T_gs of the samples cured in an oven with the T_gs of the samples cured during the first DSC scan, it can be concluded that the isothermal protocol of curing leads to more perfect network structures than the dynamic curing in the DSC. Therefore, the protocol of two isothermal steps (2 h 120 °C + 1 h at 180 °C) can be seen as a main cure step followed by a postcuring that helps to reach the best physical characteristics of the epoxy network, such as ultimate cross-link density and higher T_g [9].

Regarding the effect of graphene on T_g, it is obvious that in samples dynamically cured in the DSC, the presence of GNPs conduces to a lower T_g of the epoxy network. This agrees with the lower cross-linking degree for samples containing GNPs as it was deduced from ΔH results. However, the T_g reduction is minimized in the samples cured through two isothermal steps.

DMTA of cured GNP/epoxy nanocomposites and neat DGEBA–DDM thermoset

DMTA curves (E'-temperature and tanδ-temperature) for neat DGEBA–DDM thermoset, 1 mass% GNP/DGEBA–DDM and 5 mass% GNP/DGEBA–DDM nanocomposites at 1 Hz are shown in Fig. 3. As it can be observed, the nanocomposite with 5 mass% of GNPs presents an increased storage modulus in the glassy ($T < T_g$) and

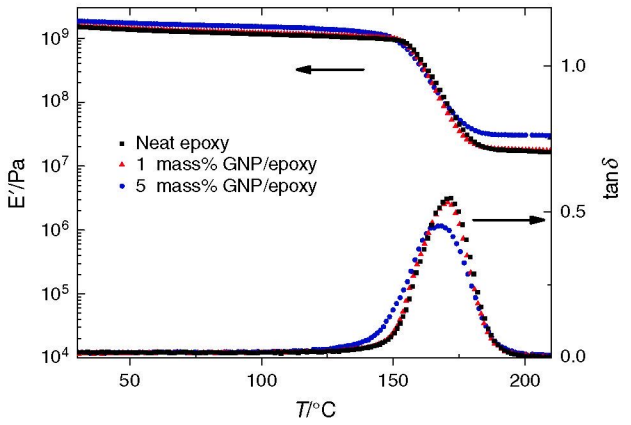

Fig. 3 E'-temperature and tanδ-temperature curves (1 Hz) for epoxy thermoset and for 1 mass% GNP/DGEBA–DDM and 5 mass% GNP/DGEBA–DDM nanocomposites

Table 3 Relative modulus $E'_{relative} = E'_{sample}/E'$ DGEBA–DDM at $T = 50$ °C (glassy region) and at $T = 190$ °C (rubbery region) and $\tan\delta_{max}$ at 1 Hz for neat epoxy thermoset and GNP/epoxy nanocomposites

Sample	$E'_{relative}$ 50 °C (glassy)	E'_{sample} 190 °C (rubbery)	$\tan\delta_{max}$/°C
Epoxy (DGEBA–DDM)	1.0	1.0	172
1 mass% GNP/DGEBA–DDM	1.0	1.0	171
5 mass% GNP/DGEBA–DDM	1.3	1.7	168

rubbery region ($T > T_g$) with regard to neat epoxy resin [$E'_{50°C}$ (neat epoxy) = 1.3 ± 0.1 GPa, $E'_{50°C}$ (5 mass% GNP) = 1.7 ± 0.1 GPa and $E'_{90°C}$ (neat epoxy) = 18 ± 2 MPa, $E'_{90°C}$ (5 mass% GNP) = 31 ± 3 MPa]. Table 3 shows the values of the relative storage modulus: $E'_{relative} = E'_{sample}/E_{DGEBA-DDM}$ at $T = 50$°C (glassy region) and at $T = 190$ °C (rubbery region). The nanocomposite with 5 mass% of GNPs presents increased glassy and rubbery moduli with regard to neat epoxy thermoset, being the increment 30 % at 50 °C and 70 % at 190 °C, respectively. However, for the nanocomposite containing 1 mass% of GNPs, the increase in E' is imperceptible, and the differences with the corresponding values of the neat epoxy thermoset are within the experimental error [$E'_{50°C}$ (neat epoxy) = 1.30 ± 0.1 GPa $E'_{50°C}$ (1 mass% GNP) = 1.36 ± 0.1 GPa]. These results agree with the previously reported for a nanocomposite containing 0.5 mass% of graphene using a different manufacturing technique [4]. Actually, higher increments on moduli would be expected on base of the very high modulus of graphene (~1 TPa); thus, these results may suggest a weak interphase between the nanofiller and the epoxy matrix.

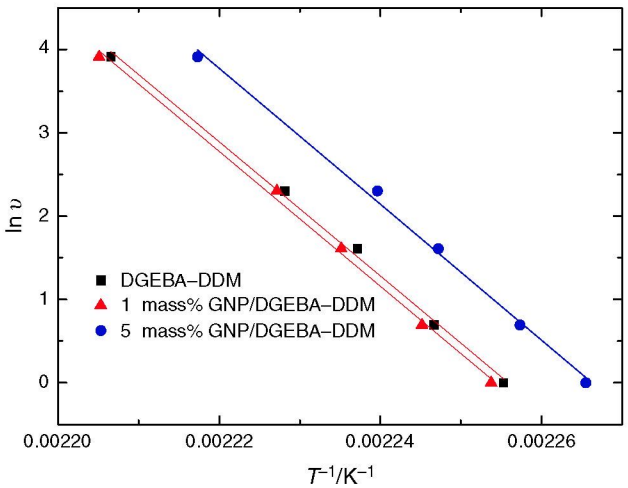

Fig. 4 Arrhenius plot for the α-relaxation of epoxy thermoset and for 1 mass% GNP/DGEBA–DDM and 5 mass% GNP/DGEBA–DDM nanocomposites

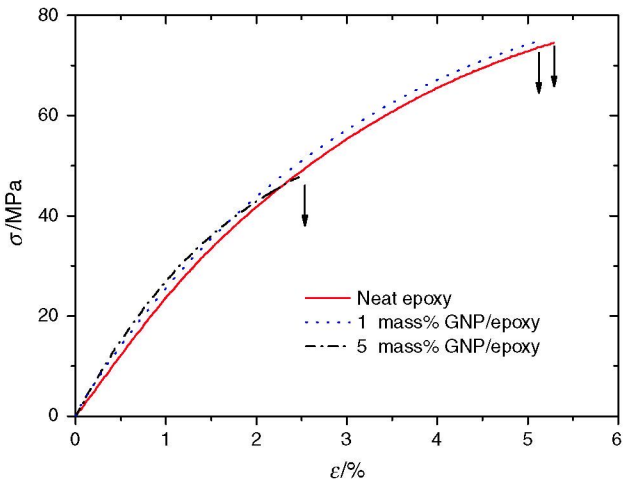

Fig. 5 Stress–strain curves for epoxy thermoset and for 1 mass% GNP/DGEBA–DDM and 5 mass% GNP/DGEBA–DDM nanocomposites

The temperature of $\tan\delta_{max}$ at 1 Hz (α-relaxation associated with the glass transition) for the neat epoxy thermoset and for the nanocomposites is also included in Table 3. These values are in agreement with those determined from DSC (see Table 2). As usual, the T_gs from $\tan\delta_{max}$ at 1 Hz are higher than the T_gs from DSC. The lower values of the temperature of $\tan\delta_{max}$ in the nanocomposites, in relation to neat epoxy thermoset, indicate a lower cross-linking density and a higher mobility of the polymer chains in the nanocomposites.

The activation energy of the glass transition relaxation (E_{aGT}) is the energy barrier that must overcome the occurrence of molecular motions causing the transition. Although it is known that the glass transition follows a

Table 4 Stress–strain results for epoxy thermoset and GNP/epoxy nanocomposites

Sample	Young's modulus/GPa	Tensile strength/MPa	Strain at break/%	Toughness from tensile curve/MJ m^{-3}
Epoxy (DGEBA–DDM)	2.50 ± 0.08	69 ± 2	4.4 ± 0.4	2.3 ± 0.5
1 mass% GNP/DGEBA–DDM	2.74 ± 0.06	71 ± 2	4.5 ± 0.5	2.0 ± 0.4
5 mass% GNP/DGEBA–DDM	3.20 ± 0.15	42 ± 5	2.0 ± 0.4	0.60 ± 0.1

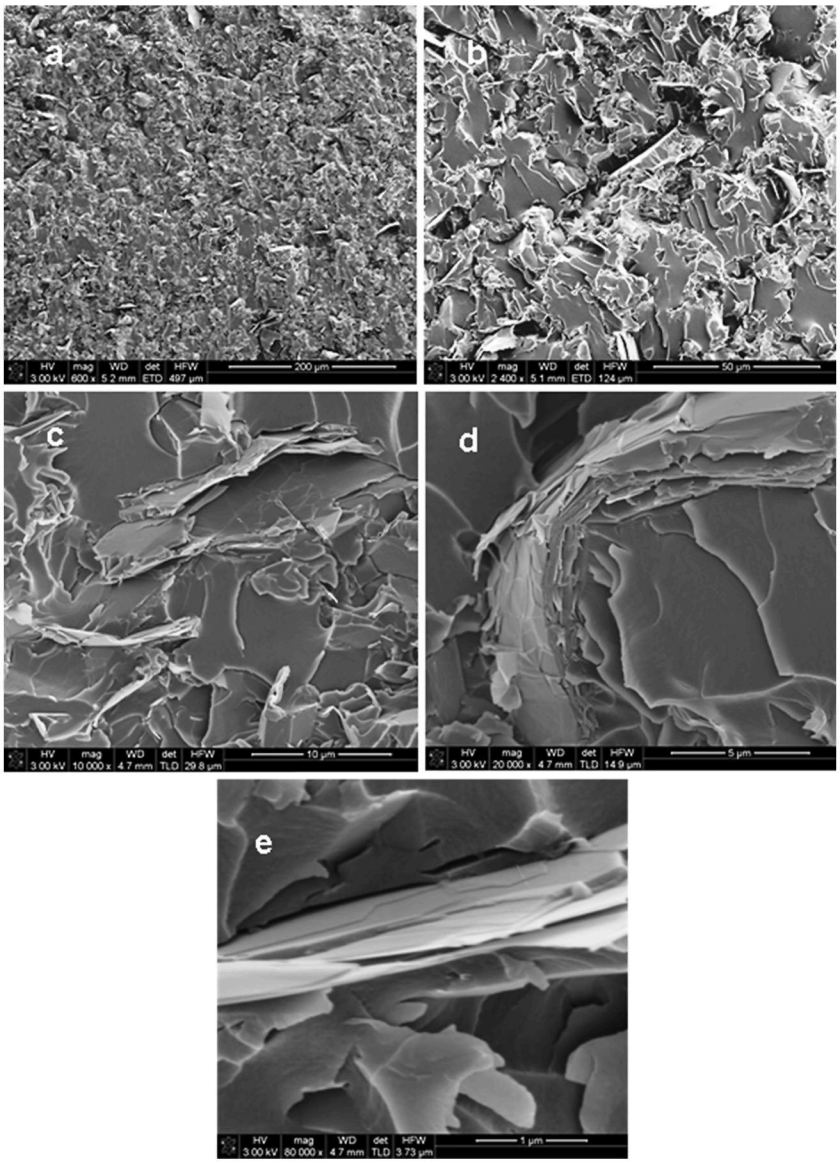

Fig. 6 SEM micrographs of 5 mass% GNP/DGEBA–DDM nanocomposite at different magnifications

Vogel–Fulcher–Tammann–Hesse behavior [19], Arrhenius equation could be used in the range of frequencies studied to evaluate the apparent value of E_{aGT}. As expected, the T_gs determined by $\tan\delta_{max}$ increase as a function of frequency (ν). Figure 4 shows the plot of ln ν versus T_g^{-1} for the neat epoxy thermoset and for the nanocomposites containing 1 and 5 mass% of GNP. From the slopes, the activation energy was calculated: 670 ± 20, 670 ± 20 and 680 ± 20 kJ mol^{-1} for neat DGEBA–DDM, 1 mass% GNP/DGEBA–DDM and 5 mass% GNP/DGEBA–DDM, respectively. Therefore, the activation energy of the glass transition relaxation

does not depend on the graphene content at least in the studied concentration range.

Mechanical tensile properties of GNP/epoxy nanocomposites

The tensile properties of nanocomposites were determined by stress–strain measurements in tensile loading. Figure 5 shows the stress–strain curves for neat DGEBA–DDM thermoset and for 1 and 5 mass% GNP/DGEBA–DDM nanocomposites. As it can be seen, the three compositions show linear behavior only at low strain. The stress–strain curves evidence that the samples exhibit fragile behavior. The values of tensile modulus (E), tensile strength (stress at break), strain at break and area under stress–strain curves, which is a measure of the toughness, were calculated from the stress–strain curves. The tensile test results which represent average values from six test samples are given in Table 4. It is worth noting that, as usual, the values of tensile modulus are higher than the values of the storage modulus [20], but the trends are similar. The data reveal that increasing GNPs content increases the modulus of the nanocomposites: 10 % increment for 1 mass% GNP and 28 % increment for 5 mass% GNP, which agrees with the DMTA results above discussed. Similar behavior has been reported for others graphene/epoxy nanocomposites [21].

However, the tensile strength values show a decrease with the increase in GNPs content. In a composite material, an increase in strength is expected when strong adhesion takes place between components and no defects are present; thus, the simultaneous decrease in tensile strength and increase in modulus of GNP/epoxy nanocomposites suggest the presence of defects due to the graphene load. The strain at break and toughness of epoxy are almost unchanged with the addition of 1 mass% of GNPs, but show a significant decrease with the addition of 5 mass% GNP. A decrease in toughness has been reported for low graphene (2 mass%) content in another graphene/epoxy nanocomposite [22].

The results here reported show that the presence of 1 mass% GNP improves the mechanical behavior of the nanocomposite while increasing GNPs content up to 5 mass% embrittles the epoxy thermoset.

SEM of GNP/epoxy nanocomposite

In order to analyze how the mechanical behavior of the 5 mass% GNP/epoxy nanocomposite was observed by SEM (Fig. 6), in order to analyze whether there is a relation between its morphology and mechanical behavior. A suitable dispersion of nanoparticles into the epoxy matrix is observed, and the graphene is homogenously dispersed (Fig. 6a). The micrographies at higher magnification evidence packaging of parallel nanoplatelets (Fig. 6c–e), thus corroborating that the graphene is not exfoliated or intercalated according to previous work [4]. The packaging of the graphene nanoplatelets would explain that the increase in the Young's modulus is not as expected. It is interesting to note that some of the nanoplatelets are wrinkled (Fig. 6d) and are debonded from the matrix (Fig. 6b). The graphene nanoplatelets deflect crack propagation [23]. Unfortunately, this fracture mechanism does not induce toughening of these composites, probably due to the weak interface. In fact, some hollows or regions with poor adhesion can be observed in the micrographs (Fig. 6b, d) that can explain the brittle behavior of these samples.

Conclusions

The incorporation of 5 mass% of GNPs accelerates the curing reaction of DGEBA–DDM; however, this catalytic effect is not detected for low graphene content (1 mass%). 1 mass% GNP/DGEBA–DDM dispersion presents exothermal peaks of reaction located at slightly higher temperatures than those of neat epoxy. The opposite effect detected for 5 mass% GNPs can be attributed to the higher thermal conductivity of this sample, which overcomes the delay effect of the GNPs steric hindrance.

In the presence of GNPs, the curing reaction becomes less exothermic and the T_g of nanocomposites lowers. GNPs hinder the epoxy-amine reaction, leading to less perfect networks than neat DGEBA–DDM thermoset. The apparent activation energy does not show an undoubted dependence with the content of GNPs.

The protocol of curing with two isothermal steps leads to more perfect network structures (higher T_g) than the dynamic curing protocol in the DSC. The T_g reduction is minimized in the samples cured through two isothermal steps.

The nanocomposite with 5 mass% of GNPs presents increased storage moduli with regard to neat epoxy thermoset, both in glassy and rubbery regions. The activation energy of the glass transition relaxation does not depend on the graphene content.

The presence of 1 mass% of GNPs slightly improves the rigidity of the nanocomposite, as reveals the elastic modulus, maintaining the other mechanical properties, tensile strength and strain at break. Increasing GNPs content to 5 mass% increases the tensile modulus at room temperature of the nanocomposite. Tensile strength decreases with the increase in GNPs content that suggests the presence of defects due to the GNPs addition. Strain at break and toughness are almost unchanged with the addition of 1 mass% of GNPs, but show a significant decrease when

the GNPs content increases up to 5 mass%. This behavior is corroborated by the morphology of the nanocomposite studied by SEM.

Acknowledgements The authors acknowledge the financial support from the Ministerio de Economía y Competitividad of Spain. Project MAT2013-46695-C3.

References

1. Hu K, Kulkarni D, Choi I, Tsukruk V. Graphene-polymer nanocomposites for structural and functional applications. Prog Polym Sci. 2014;39:1878–907.
2. Kuilla T, Bhadra S, Yao D, Kim NH, Bose S, Lee JH. Recent advances in graphene based polymer composites. Prog Polym Sci. 2010;35:1350–75.
3. Prolongo SG, Jiménez-Suárez A, Moriche R, Ureña A. In situ processing of epoxy composites reinforced with graphene nanoplatelets. Compos Sci Technol. 2013;86:185–91.
4. Prolongo SG, Jiménez-Suárez A, Moriche R, Ureña A. Graphene nanoplatelets thickness and lateral size influence on the morphology and behavior of epoxy composites. Eur Polym J. 2014;53:292–301.
5. Monti M, Rallini M, Puglia D, Peponi L, Torre L, Kenny JM. Morphology and electrical properties of graphene–epoxy nanocomposites obtained by different solvent assisted processing methods. Compos A. 2013;46:166–72.
6. Díez-Pascual AM, Naffakh M, Marco C, Ellis G, Gómez-Fatou MA. High-performance nanocomposites based on polyetherketones. Prog Mater Sci. 2012;57:1106–90.
7. Gude MR, Prolongo SG, Ureña A. Effect of the epoxy/amine stoichiometry on the properties of carbon nanotube/epoxy composites. J Therm Anal Calorim. 2012;108:717–23.
8. Shiravand F, Hutchinson JM, Calventus Y. Influence of the isothermal cure temperature on the nanostructure and thermal properties of an epoxy layer silicate nanocomposite. Polym Eng Sci. 2014;54:51–8.
9. Cowie JMG, Arrighi V. Polymers: chemistry and physics of modern materials. London: Taylor & Francis Group; 2008.
10. Puglia D, Valentini L, Armentano I, Kenny JM. Effects of single-walled carbon nanotube incorporation on the cure reaction of epoxy resin and its detection by Raman spectroscopy. Diam Relat Mater. 2003;12:827–32.
11. Puglia D, Valentini L, Kenny JM. Analysis of the cure reaction of carbon nanotubes/epoxy resin composites through thermal analysis and Raman spectroscopy. J Appl Polym Sci. 2003;88:452–8.
12. Fu Y, Zhong W. Cure kinetics behavior of a functionalized graphitic nanofiber modified epoxy resin. Thermochim Acta. 2011;516:58–63.
13. Prolongo SG, Moriche R, Jiménez-Suárez A, Sánchez M, Ureña A. Advantages and disadvantages of the addition of graphene nanoplatelets to epoxy resins. Eur Polym J. 2014;61:206–14.
14. Ozawa K. Estimating isothermal life from thermogravimetric data. Bull Chem Soc Jpn. 1966;38:1881–4.
15. Costa ML, Pardini LC, Rezende MC. Influence of aromatic amine hardeners in the cure kinetics of an epoxy resin used in advanced composites. Mater Res. 2005;8:65–70.
16. Zvetkov VL, Calado V. Comparative DSC kinetics of the reaction of DGEBA with aromatic diamines III. Formal kinetic study of the reaction of DGEBA with diamino diphenyl methane. Thermochim Acta. 2013;560:95–103.
17. Miranda MIG, Tomedi C, Bica CID, Samios D. A DSC kinetic study on the effect of filler concentration on crosslinking of dyglycidylether of bisphenol-A with 4,4-diaminodiphenylmethane. Polymer. 1997;38:1017–20.
18. Vyazovkin S, Sbirrazzuoli N. Isoconversional kinetic analysis of thermally stimulated processes in polymers. Macromol Rapid Commun. 2006;27:1515–32.
19. Riande E, Díaz-Calleja R, Prolongo MG, Masegosa RM, Salom C. Polymer viscoelasticity: stress and strain in practice. New York: Marcel Dekker; 2000.
20. Sánchez-Cabezudo M, Masegosa RM, Salom C, Prolongo MG. Correlations between the morphology and thermo-mechanical properties of poly(vinyl acetate)/epoxy thermoset blends. J Therm Anal Calorim. 2010;102:1025–33.
21. Tang LC, Wang YJ, Yang D, Pei YB, Zhao L, Li YB, Wu LB, Jiang JX, Lai GQ. The effect of graphene dispersions on the mechanical properties of graphene/epoxy composites. Carbon. 2013;60:16–27.
22. Chatterjee S, Wang JW, Kuo WS, Tai NH, Salzmann C, Li WL, Hollertz R, Nüesch FA, Chu BTT. Mechanical reinforcement and thermal conductivity in expanded graphene nanoplatelets reinforced epoxy composites. Chem Phys Lett. 2012;531:6–10.
23. Wang X, Jin J, Song M. An investigation of the mechanism of graphene toughening epoxy. Carbon. 2013;65:324–33.